J. Appl. Comput. Mech., 7(2) (2021) 839-848
DOI: 10.22055/JACM.2020.35554.2682

ISSN: 2383-4536
jacm.scu.ac.ir

Shahid Chamran University of Ahvaz

Journal of Applied and Computational Mechanics

Research Paper

Impacts of Volume of Carbon Nanotubes on Bending for Carbon-Kevlar Hybrid Fabrics

Elias Randjbaran[1], Dayang L. Majid[2], Rizal Zahari[3], Mohamed T. H. Sultan[4], Norkhairunnisa Mazlan[5]

[1] Department of Aerospace Engineering, Faculty of Engineering, Serdang, Selangor, 43400, Malaysia, Email: Elias@gmx.co.uk

[2] Department of Aerospace Engineering, Faculty of Engineering, Serdang, Selangor, 43400, Malaysia, Email: DLaila@upm.edu.my

[3] Systems Engineering Department, Military Technological College, Ministry of Defence, Muscat, PO-Box 262 PC 111, Sultanate of Oman, Email: Rizal.Zahari@mtc.edu.om

[4] Department of Aerospace Engineering, Faculty of Engineering, Serdang, Selangor, 43400, Malaysia, Email: Thariq@upm.edu.my

[5] Department of Aerospace Engineering, Faculty of Engineering, Serdang, Selangor, 43400, Malaysia, Email: NorKhairunnisa@upm.edu.my

Received October 27 2020; Revised December 29 2020; Accepted for publication December 29 2020.
Corresponding author: E. Randjbaran (Elias@gmx.co.uk)

Abstract. Carbon nanotubes indicate mechanical properties ideally examined for reinforced Carbon/Kevlar hybrid fabrics in the intact specimens by SEM and EDX observations an Carbon nanotubes indicated mechanical properties that were examined for reinforced Carbon/Kevlar hybrid fabrics in the intact specimens by SEM and EDX observations and after attempting six successful ballistic impacts, at various targets' angles: normal impact (0-degree), 10-degree, 20-degree, 30-degree, and 40-degree) with the different volume of CNT% (0, 0.1, 0.3, 0.5, 0.7, 1, and 1.5) after attempting six successful ballistic impacts, at various targets' angles: normal impact (0-degree), 10-degree, 20-degree, 30-degree, and 40-degree) with the different volume of CNT% (0, 0.1, 0.3, 0.5, 0.7, 1, and 1.5). Each sample was fabricated by the same curing unit and then evaluated by the three-point bending universal testing machine model (INSTRON-3369). Flexural Stress-Strain curves under 3-points bending in CNT epoxy composite laminates calculated flexural modulus of elasticity and bending toughness at room temperature.

Keywords: Carbon nanotubes, 3-points bending, Oblique ballistic impact, Kevlar fibre, Carbon fibre, Flexural.

1. Introduction

In today's hyper-competitive technological industries, anti-penetration items have been much extensively applied for bulletproof vests, armour; moreover, orbital debris and micrometeoroid protection layers for the space vehicles, structures, and space suits [1]. Then testing on the plates after impact was interesting to conduct (in Figure 1). In literature, reinforcing composite materials were in the Boeing 787 Dreamliner's airframe [2] and more essential structure than most previous a wide variety of commercial Boeing civil aircraft models (passenger and cargo), which illustrated in Figure 2 [2-3]. Equally important, the operating design technique without applying preconceived concept encouraged Boeing specialists to determine the ideal material for explicit applications all through the airframe design [1-3]. Otherwise, the discussed airplane, the world's first significant commercial aircraft that utilizes composite materials as the essential material in its airframe design and consequently is considered as the most eco-friendly commercial airliner due to its fuel-efficiency and lighter weight as well as lower carbon emissions and energy consumption, consequently [1-4].

Carbon fibre–reinforced composite laminates are broadly utilized in the applications where remarkable mechanical properties are important in mix with weight saving, enormous carbon fibre boards, and fuselage outlines produced using them [5]. Moreover, the chance of utilizing composite fuselage cross beams is similarly used in the Airbus A350 XWB family [6]. In addition, the great extent carbon-based composite laminates can endure a wide assortment of ecological risks – introduction to ionise radiation like a tri-nuclear oxygen centred (salicylaldoximato) and sun powered radiation in space vehicles, lightning strike in airplane, dissolvable assault, and especially impact damage being probably the most widely recognized [7]. Lately, 90% of the frames of advanced marine vessels are made of composite laminates awarding strength and plan adaptability [9]. Furthermore, 90% or a greater amount of work with composite bodies that is a considerable quantity. Composite body helps lorry industries to manufacture products that are lighter in weight and also dimimshes carbon emission and thus improves petroleum products in the motor car division. [10]. besides, the high obstruction of Kevlar fibres affect and scrape area, empowers utilisation of these filaments for body protections and impact resistances in the military division [11]. Eventually, carbon composite laminates are delicate to out-of-plane loads emanating impacts during maintenance expressly instruments drops and service operations such as lightning impacts and bird strike or runway debris [5-12].

Published online: January 01 2021

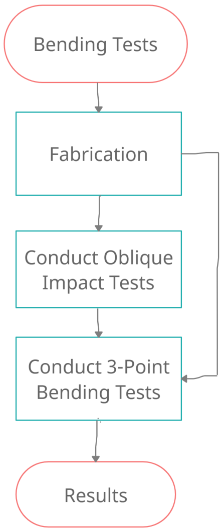

Fig. 1. Schematic configuration of conducting the tests

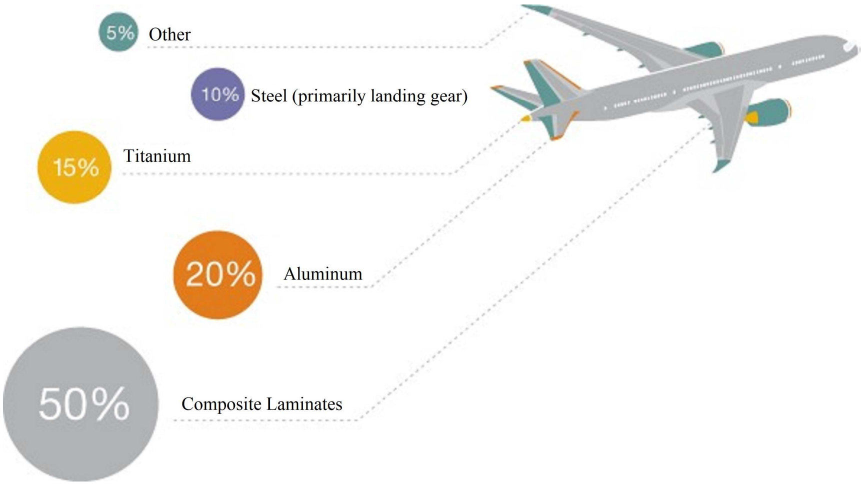

Fig. 2. Materials for Boeing 787 (Boeing report) [2-3]

Carbon/Kevlar hybrid fabrics and Carbon nanotubes (CNTs) are comprehensively adopted in structural engineering division due to their thoroughly optimised ease of fabrication and geometry, with applications as structural members in which bending is the dominant condition [13]. In the same way, flexural bending is still comprehensively adopted like the reference condition for demonstrating the bending resistance although structural members are exceptionally subject to flexural bending without calculating a moment gradient [14]. Nevertheless, experimentally, determining and comparing the toughness, flexural strength, and flexural modulus via the length of a test specimen is not straightforward to attain [15].

The three-point flexural test is performed to predict the stiffness of composite plates in bending, as an inexpensive qualitative test it is also used to evaluate both soundness of a material and the ductility. [16]. Moreover, it is a method for calculating yield properties of certain materials, measuring the ductility, and evaluating the quality of materials by their abilities to resist cracking or other surface irregularities during one continuous bend and they are assessed to obtain data about the bending properties of materials deliberated for research and development, or even for industrial operation [17-19]. Furthermore, the specimens have a tendency to fail under a similar application leading to catastrophic failure when the plates launch into fracture or utterly fractures in course of the test being valid to assume [20-22].

2. Methodology

In the current research, characterization of three-point bending properties of carbon/Kevlar reinforced epoxy composite inclusion of CNT into the matrix by varying concentrations were fabricated and after ballistic impact testing their responses were studied.

2.1 Fabrication

In reinforced composite laminates with CNT processing, CNTs were gently dispersed in a matrix of epoxy resin [22-25]. Mainly, MWCNTs type CM-95 were provided from ILJIN NanoTechnology limited company located in Seoul, South Korea [26-30]. A part of the manufacturer, the size of it was 0.01-0.015 μm of diameter and 10-20 μm of length. Incidentally, Fig. 3 displays CNT/composite laminates that were fabricated by inclusion CNT into the matrix, plus the dispersing agents were BYK 9077 (a high molecular weight copolymer with pigment affinic adhesive groups) and Araldite 2016. Besides, CNTs and BYK 9077 alongside ethanol were deliberately mixed for 5-minute, not long after followed sonication for an hour at fixed yield intensity of 25-Watt. Essentially, the blend was added and mixed 10-minute with high shear mixing homogeniser at 3500 R.P.M., trailed by 45-minute sonication treatment. Importantly, the mixture was then positioned in the vacuum degassing oven and stayed at 25°C for 48-hour under 1-Bar, trailed by 24 hours under 1-Bar at 80°C for degassing operation (in Figure 3). Meanwhile, the open moulding process in which constituents or consecutive plies of strengthening composite laminates or resin-impregnated fortifications were applied to the form and the composite was developed and worked by hand. In addition, restoring is typically directed at surrounding temperatures; however, the process could be expressly accelerated by elevating the temperature. Eventually, the hand lay-up technique relatively fabricates the substantial aggregate of reinforced composite laminates [28, 30].

2.2 Three-point flexural tests

After being demoulded, the panels were marked to prepare them for trimming. Equally important, the dimensions for trimming was as specified in ASTM D790 [31]. As a result, Figure 4 displays the schematic diagram that in accordance to the ASTM D790 Standard; the three point bend test as a classical experiment in mechanics was ecclesiastically achieved by applying the Universal Testing Machine model (INSTRON-3369), which facility utilised in this experiment was available in Department of Mechanical and Manufacturing Engineering's laboratory, Faculty of Engineering, Universiti Putra Malaysia (UPM) as reported. Consequently, the test reactions of each sorts of samples are numerically plotted. In conjunction with qualities of the after ballistic impact, neat epoxy resin composites and CNT/epoxy composite structures were lower than intact samples without any type of initial cracks. Likewise, these quality request could be clarified by the quantity of filaments crossing close to the break plane. Conjointly, it generally depicts the areas of splits got for each model and the comparing quantities of meeting strands [32]. Including, dissimilar to the fibre-based models, the work models contain a few focuses where numerous strands unite, and accordingly the comparing appropriation plots show a few pinnacles, which delineate the number of filaments across every specific plane clarifying the reasons for various estimations of qualities were acquired for various models. Accordingly, the quantity of considering filaments at the split plane of each model was relative to the composite quality [29-31].

Tabulation of data was generated and processed automatically by the Bluehill® HV Software that is specifically designed for the Instron®. In particular, flexural strength of the composite was calculated using relationship (1) [31];

$$\sigma = (3PL)\,(2bt^2)^{-1} \tag{1}$$

Consider a rectangular plate with the uniform thickness, where σ was stress in the outer specimen at midpoint (flexural strength) [MPa], P was maximum load on the load deflection curve [N], L was support span length [mm], b is width of the sample [mm], and t was thickness of the sample [mm].

The flexural modulus, E was obtained from the formula below. With this purpose in mind, the value of m was calculated by drawing a tangent to the steepest initial straight-line portion of the load-deflection curve and using the equation (2), the value of E was obtained [31] respectively, providing the following equivalence:

$$E = (mL^3)\,(4bt^2)^{-1} \tag{2}$$

where E was modulus of elasticity [MPa], L was support span length [mm], b was width of the sample [mm], t was thickness of the sample [mm], and m was slope of the tangent to the initial straight-line portion of the load-deflection curve [N.mm^{-1}].

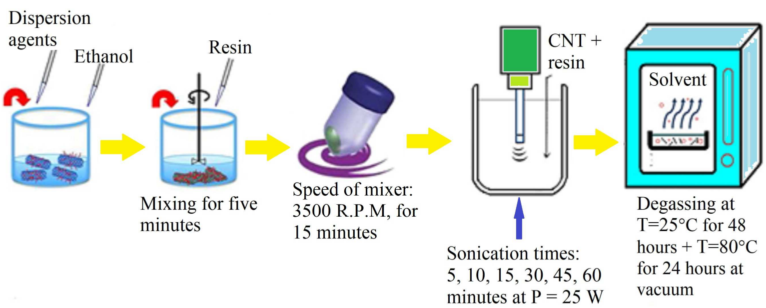

Fig. 3. Structure for the fabrication in the CNT composite laminates [29]

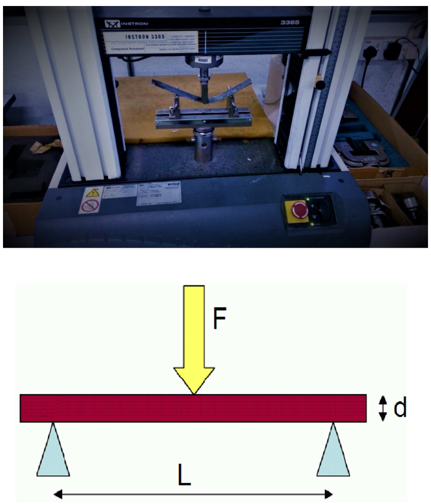

Fig. 4. A) under load specimen B) schematic of three-point bending flexural test setup following the ASTM D790 [31]

Three point bending is the most frequently applied set-up, and involves a long sample being placed on two supporting pins, a set distance apart, with a roller descending to contact the specimen midway between two supporting pins [31]. Therefore, the loading arm descends at a uniform rate to bend the specimen, first it deformed it elastically, then plastically. Finally, fracture occurred when the specimen was the force required within the limit of the load unit and sufficiently brittle.

3. Results and Discussion

Analysing needed use the SEM images and describe the graphs.

3.1 Morphology

Figure 5 shows the SEM image of a raw MWCNT. Moreover, uniform, smooth, and straight tube walls of MWCNTs are observed showing no structural defects and own high aspect (diameter/length) ratios.

The SEM inspection verify the results and observing the failure systems of deliberated composite laminates, microscopic and nanoscopic images were taken by SEM via a distinctive fracture surface. Similarly, they show the matrix debonding, microcracks and because of the strength distribution of the fibers, weak fibers are the first to fail. Furthermore, Figure 6A illustrates matrix cracking is the initial flaw occurring in composite loading. On the other hand, matrix cracking is a fracture-mechanics issue and first step of failure mechanism due to epoxy laminate is outermost layer of epoxy laminating system and first layer bearing flexural stress strength (from top to bottom of the specimens), respectively. Moreover, Figure 6B shows fiber breakages under flexural loading specimens. Fiber breakage is a last step of the composite laminates' life-cycle. Finally, Figure 6C displays debonding of matrix and fiber and vacancies of fibers at epoxy matrix.

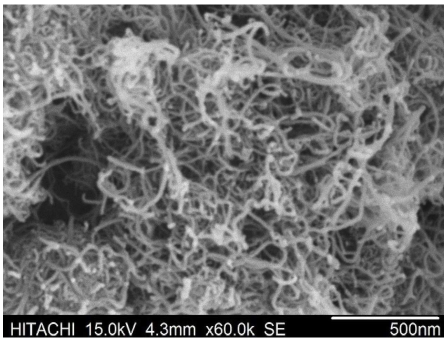

Fig. 5. MWCNTs magnified by SEM (500nm)

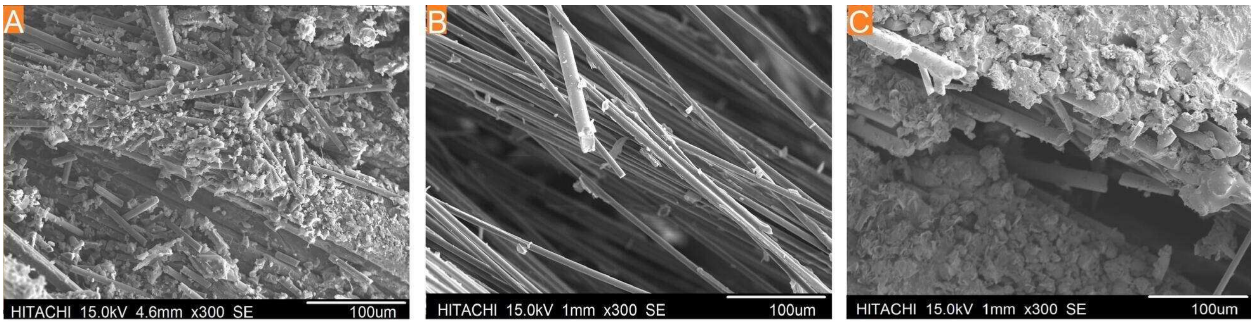

Fig. 6. Damaged samples A) dispersed 1.5% CNT on surface, B) fibre breakages, and C) debonding of matrix and fiber

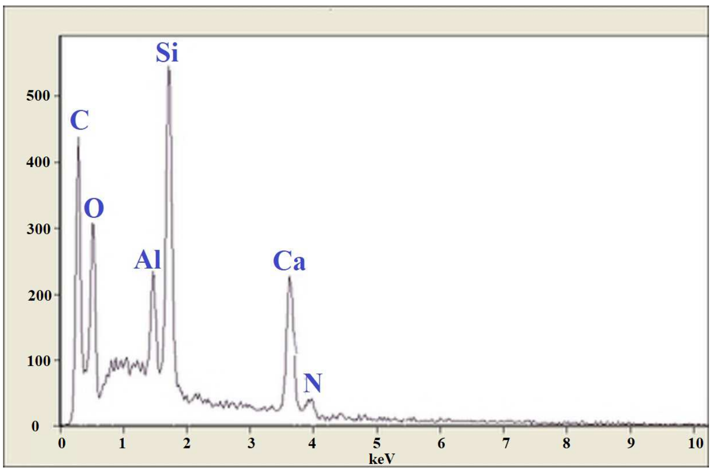

Fig. 7. The EDXMA pattern of reinforced resin with the 1.5% MWCNTs

The energy dispersive X-ray microanalysis (EDXMA) in Figure 7 observation proved the significant amount of silicon and carbon, and oxygen bonded on the side multi-walled carbon nanotubes (MWCNTs). Nonetheless, paradoxical to what was expected, probably oxygen is not only because of the existing of carboxylic acid group (-COOH) as the exchange group. Considerably, also chlorine was revealed, and its presence can be ascribed either as an impurity or as part of acyl chloride groups resulting from the functionalization process. Similarly, the lack of signals attributable to aluminium particles proposes functionalising treatment due to the removal of the catalyst particles, which is indispensable for the CNT growth. Moreover, microstructure of broke surface of specimens is investigated via the images of SEM (scanning electron microscopy) and EDXMA is performed for the specimens' chemical characterization or elemental analysis. Therefore, the spectra of energy dispersive are achieved containing Roentgen radiation beam energy (0 to 10 keV) then indicating in X-axis and number of counts per second, CPS, indicating in Y-axis at 35-degree. In fact, spectra are generally set at the points in SEM images, at this specific point compound piece is large diagnostically attained. Lastly, the incident beam energizes an electron in an internal shell then catapulting it from the shell. Finally, the lower energy shell can be delivered as a Roentgen radiation beam energy being normal for the distinction in energy between the dual shells while making an electron-hole filling by an electron from an external (the highest level of energy) shell and the distinction in energy among the higher ones.

3.2 Calculations and plots' interpretations

Figures 8-14 demonstrate the intact specimens and after attempting six successful ballistic impacts, at various targets' angles (present six different results on Effects of Volume of Carbon Nanotubes on the Angled Ballistic Impact for Carbon Kevlar Hybrid Fabrics [29]: normal impact (0-degree), 10-degree, 20-degree, 30-degree, and 40-degree) with the different volume of CNT, which added into epoxy resin including 0, 0.1, 0.3, 0.5, 0.7, 1, and 1.5 percent. In these single line graphs, X-axis indicates flexural strain (in per-cent) and Y-axis indicates flexural stress in mega Pascal (MPa).

The line graph in Figure 8 illustrates Flexural stress-strain curves in Neat Epoxy/Carbon-Kevlar hybrid fabrics, after oblique impacts between 0 and 40 degrees and intact sample. Overall, all maximum points of stress and strain of flexural bending have steadily declined by increasing the angles of impact. Then the latter has slumped or collapsed since reaching to maximum level of stress while the downturn for the former began in 0 as stress and different levels of the strain. However, there has been a sharp rise in crack initiation since multiple fibre fracture events. In composite plates, the maximum values of bending stress and strain were of 0-degree at 16.03MPa and 2.26% strain, 10-degree at 14.52 and 2.54% strain, 20-degree at 13.5MPa and 2.04% strain, 30-degree 11.99MPa and 1.81% strain, 40-degree at 10.94 MPa and 1.39% strain, plus intact at 3.23MPa and 3.23% strain. Moreover, although the flexural strength (maximum moment) of intact sample and after 40-degree impact one had dropped, it only represented 74.3% decrease. As the flexural strength began to fall in all impacted samples, in intact sample started to rise. It rose steadily and the flexural strength in strain by 3.23%. During the same strain from 0% to 1.3%, 40-degree sample reaching to maximum and substantially shrank, but then rest of them started to grow more dramatically. 20-degree impact sample in 12.61 MPa at 1.73% of strain the multiple fibre fracture events started and inflated, but fell to 13.5 MPa by 2.04%. This was slightly higher than 30-degree impact sample, which shrank to 11.99 MPa and 1.81%. 0-degree impact sample on the other hand, overtook other impact samples and accounted for just over 16.03 MPa of flexural strength in 2.26% strain.

The line graph in Figure 9 compares the three-point bending flexural test on various composite intact and after oblique impact from 11.43 and 29.35 MPa of the bending strength, plus between 2.11% and 3.33% of flexural strain. Overall, the value of stress and strain of 40-degree impact declined over the 2.11% of strain, whereas the amount of intact sample that increased at the same point. Moreover, in 2.403% of strain, the highest value of the bending strength with intact sample was 27.78 MPa, being valued 2.06 times of 20-degree, 1.89 times of 10-degree, 1.67 times of 0-degree impacted samples. Consequently, this was far less than maximum stress value of 40-degree impact sample, which were reached approximately 2.6 times. However, apart from a brief rise from 2.63% to 2.97%, and the value of bending strength in 20-degree impact sample gradually declined over the 2.632% strain to collapse at just under 13.7 MPa. In sharp contrast to this, intact sample valued the others at much higher levels. the bending strength values increased gradually until they broke; intact at 29.35 MPa, 0-degree impact at 16.95 MPa, 10-degree at 15.04 MPa, 20-degree at 13.69 MPa, 30-degree at 12.18 MPa, and 40-degree at 11.43 MPa. Notwithstanding, they then levelled off from 2.11% to 3.33%. After rising, crack initiation since multiple fibre fracture events, soon after they collapsed.

The line graph in Figure 10 shows the three-point bend testing behaviour of carbon-Kevlar fibre-reinforced composite laminates from 0-4% strain. Overall, the intact sample has been the dominant type and continues up to the fracture point with 33.05 MPa at 4.05% strain. After impact samples have represented a small and not significant proportion of total stress use and despite small projected gains compare the intact sample; it is projected they continue dropping so. After 40-degree impact commands the lowest amount of stress strength with 10.99 MPa in 2.49% strain, at the same point on 30-degree impact sample rising to approximately 12.34 MPa in 2.41% strain to break and current trend is set to gradually continue with a projected ultimate stress value of the others. Respectively, in 3.61% strain, 0-degree impact (normal impact) sample came in second, with 18.06 MPa stress strength. However, intact sample overtook impact sample in all aspects and despite some fluctuations were crack initiation since multiple fibre fracture events after yield point.

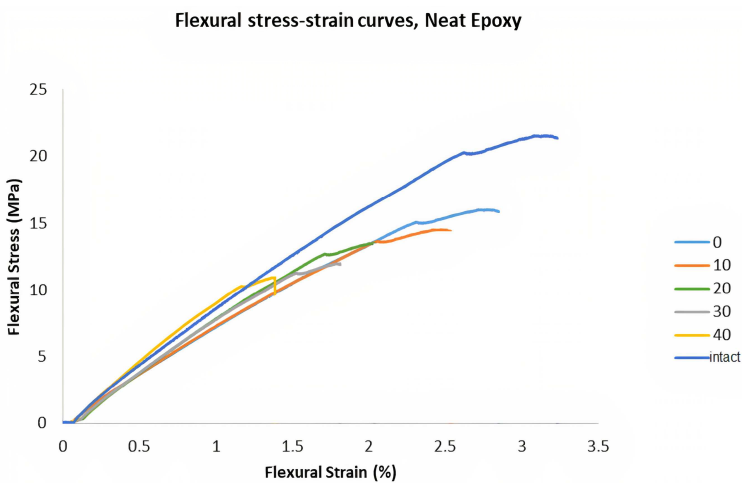

Fig. 8. Flexural Stress-Strain curves under 3-points bending in neat epoxy composite laminates at room temperature

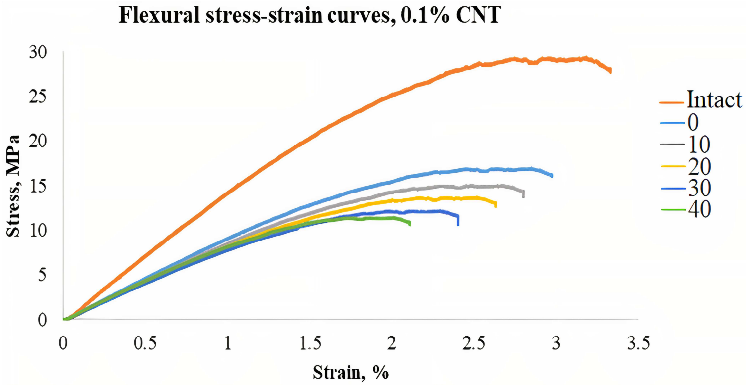

Fig. 9. Flexural Stress-Strain curves under 3-points bending in 0.1% CNT epoxy composite laminates at room temperature

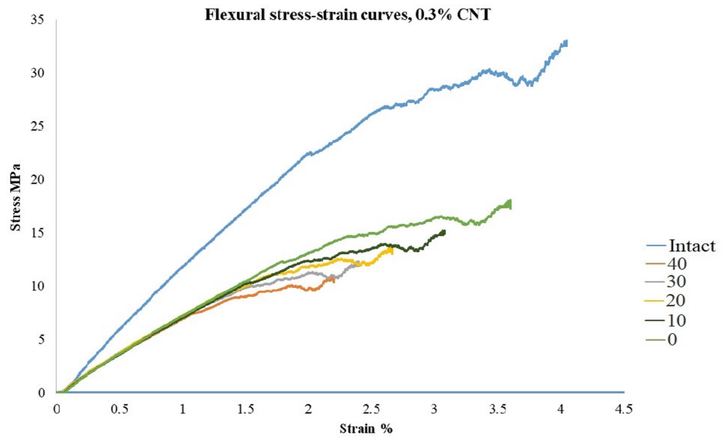

Fig. 10. Flexural Stress-Strain curves under 3-points bending in 0.3% CNT epoxy composite laminates at room temperature

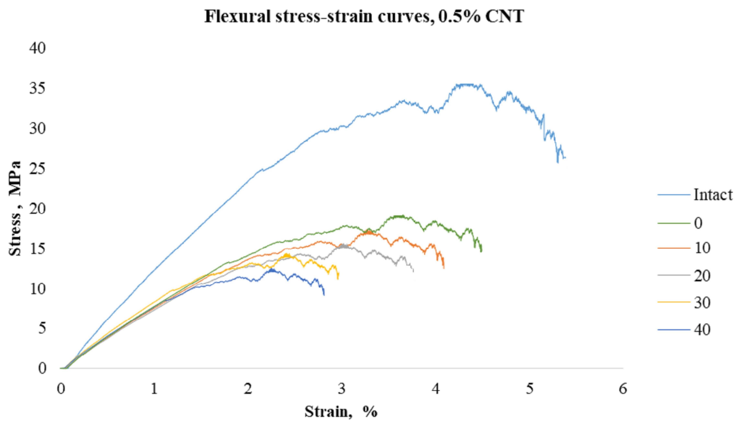

Fig. 11. Flexural Stress-Strain curves under 3-points bending in 0.5% CNT epoxy composite laminates at room temperature

The line graph in Figure 10 shows the three-point bend testing behaviour of carbon-Kevlar fibre-reinforced composite laminates from 0-4% strain. Overall, the intact sample has been the dominant type and continues up to the fracture point with 33.05 MPa at 4.05% strain. After impact samples have represented a small and not significant proportion of total stress use and despite small projected gains compare the intact sample; it is projected they continue dropping so. After 40-degree impact commands the lowest amount of stress strength with 10.99 MPa in 2.49% strain, at the same point on 30-degree impact sample rising to approximately 12.34 MPa in 2.41% strain to break and current trend is set to gradually continue with a projected ultimate stress value of the others. Respectively, in 3.61% strain, 0-degree impact (normal impact) sample came in second, with 18.06 MPa stress strength. However, intact sample overtook impact sample in all aspects and despite some fluctuations were crack initiation since multiple fibre fracture events after yield point.

The line graph in Figure 11 illustrates the number of flexural stress–strain curves received by the three-point bending flexural tests according to the type of flexural stress and strain in the intact and impact samples from 0 to 5.5% strain. Although the main reason for breaking, indicated lower energy absorption characteristics or brittleness of samples by performing a bending test at the breaking point. However, the intact sample owned the largest amount of flexural stress in relation to the bending. During the test, the figure for the samples steadily increased and reached the highest points for 0-degree at 19.48, for 10-degree at 17.37, for 20-degree at 15.61, for 30-degree at 14.38, for 40-degree at 12.51, and for the intact at 36.57 MPa flexural stress. Beginning with yield points then the cracks initiation in different points, the value of bending strain in regard to the composition of materials based on level of CNT into the resin between 0 and 4.32%, stress slightly went up from 12.51 to 19.49 MPa before experiencing a dramatic rise to the peak of approximately 3 times less than intact sample. On the other hand, the value of stress steeply increased in the intact sample at 12.51 MPa, since that value rest of them went up reasonably stable during the same value. The last noticeable item in 30-degree impact sample, the value of stress caused by bending stabilized in going up until it broke to a low point of 14.38 MPa till 2.41% strain, then it and continued to incline steadily until breaking.

The displayed line graph in Figure 12 illustrates the values of stress-strain curves in the three-point bending flexural tests between 0 and 5.85% strain. Overall, the value of failure stress obtained by three-point bending developed at first and declined at culmination with a stable trend. Since it is observed in the graph of 40-degree impact, the value of failure stress was only about 12.74 MPa in 0.66% strain. By decreasing the angles of target, the value of failure stress improved slowly from 14.67 MPa to 19.76 MPa between 1.4% and 2.66% strain. In intact sample, from 0 to about 5% strain, the stress' value boomed from 0 to 37.55 MPa. For 0-degree impact sample, there was no change at all in term of trend from 0 to breaking point of the rest of impact samples. The intact sample compares with the 0-degree impact, the value of failure stress went down rapidly from 37.55 MPa to 19.76 MPa, i.e., 1.9 times greater. At the end of the breaking of all of them, the value of stress plummeted from 37.55 MPa (for the sample of intact) to 12.74 MPa (for the sample of 40-degree impact), i.e., 2.95 times stronger than 40-degree sample. In fine, the graph shows the highest value of failure stress tested for the samples of impact is 19.76 MPa while the lowest one is 12.74, i.e., 0-degree sample is 1.56 times more stable than 40-degree sample.

The line graph in Figure 13 compares the number of three-point bending test for six different samples in intact and impact samples from 0% to 6% strain. Overall, it can be seen tensile strength was far higher in intact sample than in the other five samples throughout the flexural. To begin, the stress at failure in bending of in 0, 10, 20, 30, and 40-degree samples, followed a fairly similar pattern over the yield points. The general trend though for the impact samples was a decline in the values of strength stress over the breaking points. In contrast, intact experienced an upward trend, starting at approximately 2% strain, and breaking at just 6.07%. Interestingly, strength stress in 40-degree impact sample reached at 13.83 MPa, which far less than intact sample, which is about 3 times less than intact one. They then fluctuated over the yield points, reaching a peak and breaking slightly lower than intact one.

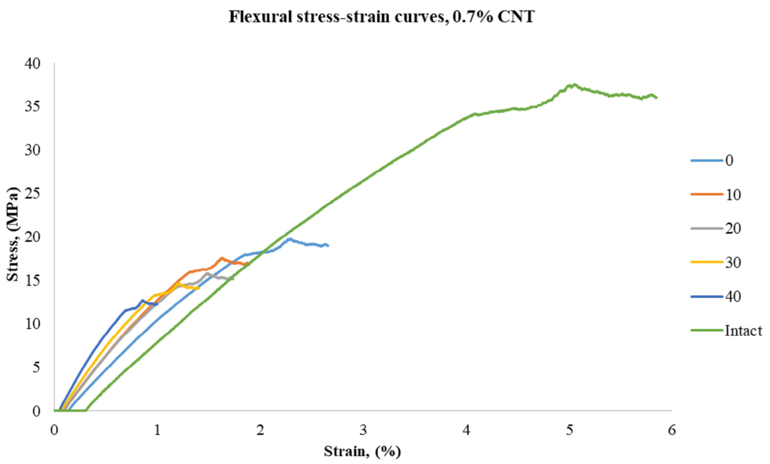

Fig. 12. Flexural Stress-Strain curves under 3-points bending in 0.7% CNT epoxy composite laminates at room temperature

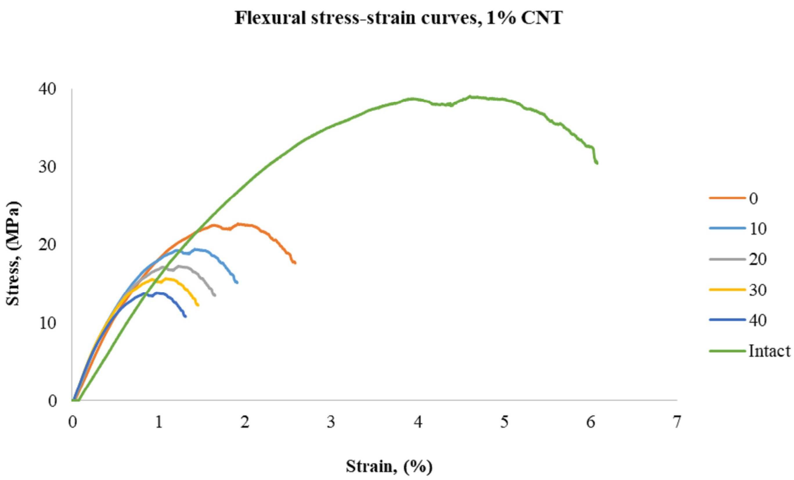

Fig. 13. Flexural Stress-Strain curves under 3-points bending in 1% CNT epoxy composite laminates at room temperature

Figure 14 compares changes in the three-point flexural bend tests distribution among the six different samples from 0 to about 6.34% strain. The only sample where the maximum value of bending stress is expected to increase by 43.05 MPa is the intact sample, while 40-degree sample is expected to have the greatest drop in value of flexural stress over the bending test. Also, the all samples are showing the fluctuations once reaching to the flexural strength until breaking. Equally important, from a relatively small values of strain for typical of the impact samples from 0.78% to 1.302%, i.e., by decreasing the angles the maximum difference can be about 66%. Further, for 0-degree sample, breaking point is 2.82%, about 16% more than 10-degree impact, then maximum of stress is 33.9 MPa, about 36% more than 10-degree. Besides, this is almost a reversal of the situation for 30 and 40-

degree impact samples, which stood at 16.67 and 14.66 MPa in 1.86% and 1.62% strain. Moreover, it is expected to continue its steady decline to reach the breaking points. In addition, another notable trend can be seen in the data for the samples, which is the region of strain at the maximum of bending stress to show an increase in all over the testing. Nevertheless, the prediction of a decline, albeit small, looking forward to breaking. Finally, these results reflect those of Mohsen et al. (2017) who also found the results in the flexural Stress-Strain curves indicate the integration of CNTs into the system had a statistically significant effect on the flexural strengths.

The bar graph in Figure 15 illustrates the modulus of bending tests, which conducting in hybrid with different value of CNT on six types of samples; intact and after impact. In terms of angled target impact and the CNT volume fraction, neat epoxy owned the most at 10.25 GPa. The ratio of stress to strain in flexural deformation for 1.5% CNT after 10-degree impact was the highest one (59.11 GPa) compared to the 0.1% CNT after 10-degree impact, which acquired the least (8.61 GPa). For 1% CNT, at normal (0), 30, and 40 degrees possessed about 30 GPa and 10-degree is nearly 40% more than the intact one, respectively. On the other hand, the lowest flexural modulus was on 0.1% CNT at 20 and 30-degree, which accounted for nearly 8.3 GPa in all the samples. The 0.3% CNT at the intact one had most on these items at just 16.71 GPa that is around 73% of 40-degree (9.68 GPa). For 0.7% CNT, 40-degree specimen was doubled he intact one, 70% more than normal impact, about 40% more than 10 and 20-degree impact, 22% more than 30-degree impact. Otherwise, for 0.5% CNT, the difference between maximum and minimum of this category is about 71%. Overall, the category of 1.5% CNT that all specimens acquired high level of bending modulus, which was about five times higher than on the average of neat epoxy.

Bar graph in Figure 16 illustrates some interesting results about some toughness of composite laminates with and without CNT after impact and intact from three-point bending specimens. In addition, they allow comparisons between specimens owning different CNT amount versus intact and after oblique impact, and shows specimens possessing of the highest and the lowest value toughness. Besides, the intact specimen with 1.5% CNT is striking at over 218 J.m^{-3}. Additionally, specimens with 0.1% of carbon compared to the other specimens showing the second toughest samples to break due to the toughness value from 13 to 175 J.m^{-3}. Furthermore, 0.7% CNT is third tough specimen, roughly triple as much as intact and double more than the normal impact with neat epoxy, which is the only sample with less energy absorbed by 8.45 J.m^{-3} than all of them. Systematically, in terms of toughness for less volume of CNT by 0.1%, intact is the toughest specimens by 64 J.m^{-3}, more than approximately double normal impact with 33 J.m^{-3}. Comparatively, 0.3% CNT is the third tough material to absorb by about 80 J.m^{-3} at the intact sample then by increasing the angle of impact the level of toughness dropped to 14 J.m^{-3}. Relatively, 0.5% CNT has over three times more than neat epoxy, double the 0.1% CNT, and 56% tougher than 0.3% CNT. Nevertheless, the toughness of 0.5% CNT is nearly 8% less than 0.7% CNT, 41% less than 1% CNT, and 76% less than 1.5% CNT for the intact samples. As for after impact, intact 40 degree impact is the least value of toughness with 8.45 J.m^{-3}. Overall, in the after-40-degree impact, 1.5% CNT shows the highest value of toughness, about four times more than the intact sample, about double the 1.0%, 0.3%, 0.7% and 1% CNT, 78% more than 0.5% CNT. However, after-20-degree impact, 1.5% CNT has by far the greatest value of toughness. Moreover, there seems to be correlation between the angle and the value of CNT.

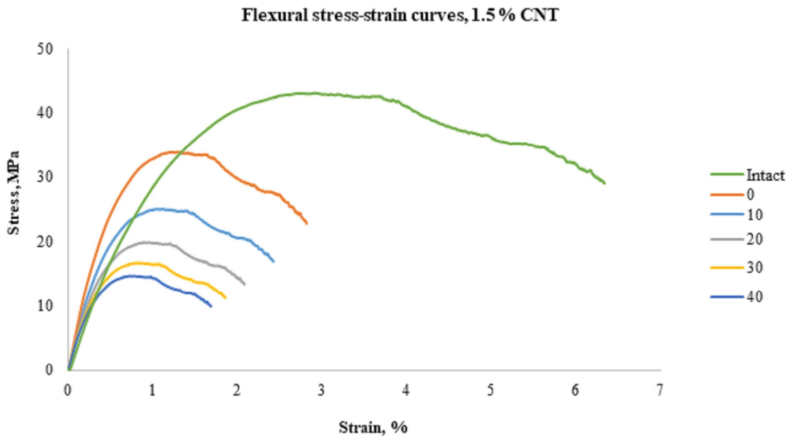

Fig. 14. Flexural Stress-Strain curves under 3-points bending in 1.5% CNT epoxy composite laminates at room temperature

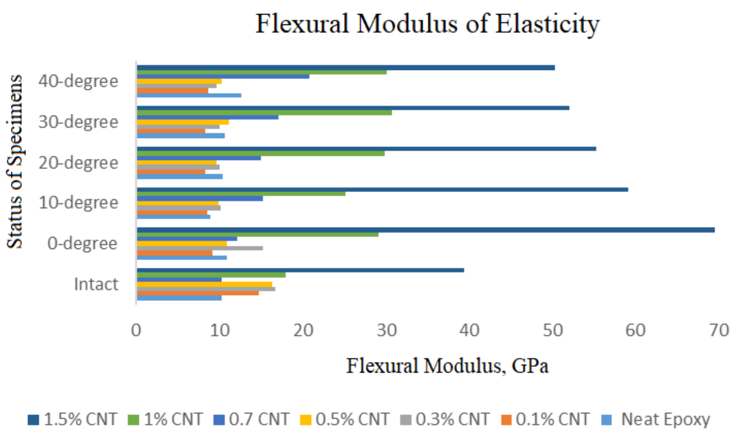

Fig. 15. Flexural modulus of elasticity for the specimens

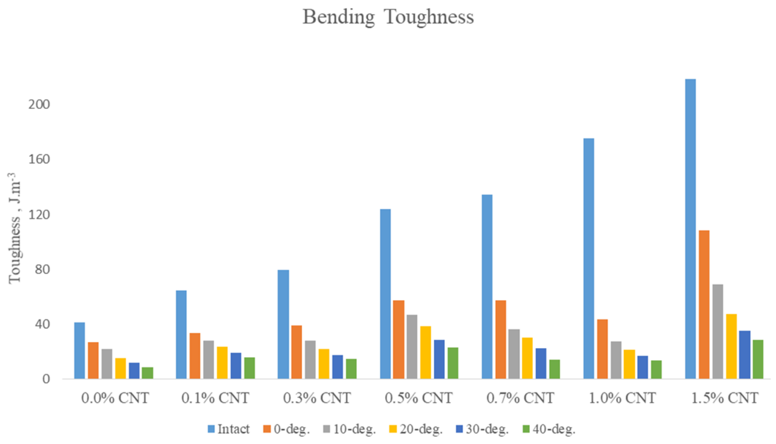

Fig. 16. bending toughness of the specimens

4. Conclusions

Briefly, current work considered the flexural strength of reinforced Carbon/Kevlar hybrid fabrics affected by impact damage and compare it to the strength of the intact specimen. The results presented a number of Flexural Stress-Strain curves under 3-points bending for different volumes of CNT epoxy composite laminates at room temperature. Moreover, the elasticity modulus and bending toughness of the specimens were calculated. Based on the outcomes, the flexural mechanical behaviour of composite laminates reinforced with CNT in impact damage and intact mode, it may be concluded: with addition of CNT into the epoxy, as a filler, there was an increase of the modulus of elasticity and a reduction of the angle of ballistic impact limit. Intact specimens repeatability presented in the results indicated a magnificent process of fabrication.

- For the intact samples of the neat epoxy composite laminates (10 MPa and 41 $J.m^{-3}$), the flexural strength and toughness was increased compared to the CNT inclusion in the system, 1.5% CNT (59 MPa and 218 $J.m^{-3}$). In addition, after ballistic impact damage, the flexural properties for the reinforced Carbon-Kevlar® hybrid fabrics laminate with even the highest volume of CNT (1.5%) exhibited a reduction of the flexural modulus and the maximum flexural stress when the fibre fracture was increased due to the impact damage, in the range of 0 to 40 degrees analytically examined.
- For future works, it is requisite to accomplish flammability experiments to verify the efficacy of the efficacy in decreasing the flame extinction duration and the rate of flame propagation, substantiating the possibility of using the reinforced composite with CNTs in interiors of civil aircraft.

Author Contributions

E. Randjbaran planned the scheme, initiated the project, and suggested the experiments; D.L. Majid and R. Zahari conducted the experiments and analyzed the empirical results; M.T.H. Sultan and N. Mazlan developed the mathematical and examined the validation. The manuscript was written through the contribution of all authors. All authors discussed the results, reviewed, and approved the final version of the manuscript.

Acknowledgments

The authors would like to thank to Universiti Putra Malaysia (UPM), especially the Department of Aerospace Engineering, and the Ministry of Education, Malaysia.

Conflict of Interest

The authors declared no potential conflicts of interest with respect to the research, authorship, and publication of this article.

Funding

The authors received financial support for the research, authorship, and publication of this article as a part of the research done within the project code FRGS/1/2019/STG07/UPM/02/10 and VOT No. 5540209.

References

[1] Manyapu, K. K., De Leon, P., Peltz, L., Gaier, J. R., Waters, D., Proof of concept demonstration of novel technologies for lunar spacesuit dust mitigation, *Acta Astronautica*, 137, 2017, 472-481.
[2] Pandian, G., Pecht, M., Zio, E., Hodkiewicz, M., Data-driven reliability analysis of Boeing 787 Dreamliner, *Chinese Journal of Aeronautics*, 33(7), 2020, 1969-1979.
[3] Scola, A., Eberling-Fux, N., Turenne, S., Ruiz, E., New liquid processing of oxide/oxide 3D woven ceramic matrix composites, *Journal of the American Ceramic Society,* 102(6), 2019, 3256-3268.
[4] Chudoba, B., *Generic aerospace vehicle design – knowledge utilization*, In: Chudoba, B., Stability and Control of Conventional and Unconventional Aerospace Vehicle Configurations, Springer, Cham, 2019, 19-46.
[5] Ravishankar, B., Nayak, S.K., Kader, M.A., Hybrid composites for automotive applications – A review, *Journal of Reinforced Plastics and Composites,* 38(18), 2019, 835–845.
[6] Borges, D.J., Cardoso, D.C., Braga, E.M., Castro, A.A., Dos Reis, M.A, Loayza C.R., Stainless steel weld metal enhanced with carbon nanotubes, *Scientific Reports,* 10(1), 2020, 1-3.
[7] Randjbaran E., Zahari R, Majid D.L., Sultan, M.T.H., Mazlan, N., Research paper in literature of increasing thickness by inclined target, *Elyns Journal of Material Science and Techniques*, 1(1), 2018, 104.
[8] Randjbaran, E., Zahari, R., Majid, D.L., Sultan, M.T.H., Mazlan, N., Reasons of adding carbon nanotubes into composite systems-review paper,

Mechanics and Mechanical Engineering, 21(3), 2017, 549–568.
[9] Marinkovic, D., Rama, G., Zehn, M, Abaqus implementation of a corotational piezoelectric 3-node shell element with drilling degree of freedom, *Facta Universitatis, Series: Mechanical Engineering*, 17(2), 2019, 269-283.
[10] Duchene, P., Chaki, S., Ayadi, A., Krawczak, P., A review of non-destructive techniques used for mechanical damage assessment in polymer composites, *Journal of Materials Science,* 53(11), 2018, 7915-7938.
[11] Mylsamy, B., Palaniappan, S.K., Subramani, S.P., Pal, S.K., Sethuraman, B., Innovative characterization and mechanical properties of natural cellulosic Coccinia Indica fiber and its composites, *Materials Testing,* 62(1), 2020, 61-67.
[12] Qu, J., Sun, Z., Strength behavior of shanghai clayey soil reinforced with wheat straw fibers, *Geotechnical and Geological Engineering,* 34(2), 2016, 515-527.
[13] Süsler, S., Kurtaran, H., Türkmen, H.S., Kazancı, Z. Lopresto, V., An experimentally validated numerical method for investigating the air blast response of basalt composite plates, *Mechanics of Advanced Materials and Structures,* 27(6), 2020, 441-454.
[14] Nayak, S.Y., Satish, S.B., Sultan, M.T.H., Kini, C.R., Shenoy, K.R., Samant, R., Sarvade, P.P., Basri, A.A., Mustapha, F., Influence of fabric orientation and compression factor on the mechanical properties of 3D E-glass reinforced epoxy composites, *Journal of Materials Research and Technology,* 9(4), 2020, 8517-8527.
[15] Randjbaran, E., Zahari, R., Majid, D.L., Sultan, M.T., Mazlan, N., Mechanical properties of disconnected multiwalled carbon nanotubes and carbon nanotube composites-a review paper, *International Journal of Research-Granthaalayah,* 6(6), 2018, 212-225.
[16] Wang, Z., Zhao, X. L., Xian, G., Wu, G., Raman, R. S., Al-Saadi, S., Haque, A., Long-term durability of basalt-and glass-fibre reinforced polymer (BFRP/GFRP) bars in seawater and sea sand concrete environment, *Construction and Building Materials,* 139, 2017, 467-489.
[17] Ning, F., Cong, W., Hu, Y., Wang, H., Additive manufacturing of carbon fiber-reinforced plastic composites using fused deposition modeling: Effects of process parameters on tensile properties, *Journal of Composite Materials,* 51(4), 2017, 451-462.
[18] Nayak, S.Y., Satish, S.B., Sultan, M.T.H., Kini, C.R., Shenoy, K.R., Samant, R., Sarvade, P.P., Basri, A.A., Mustapha, F., Influence of fabric orientation and compression factor on the mechanical properties of 3D E-glass reinforced epoxy composites, *Journal of Materials Research and Technology,* 9(4), 2020, 8517-8527.
[19] Dhand, V., Mittal, G., Rhee, K. Y., Park, S. J., Hui, D., A short review on basalt fiber reinforced polymer composites, *Composites Part B: Engineering,* 73, pp. 166-180.
[20] Prasad, P.R., Prakash, J.N., Manjunath, L.H., Reddy, P.V., 2020, Physical and wear properties of UHMWPE fabric reinforced epoxy composites, *International Journal of Automotive and Mechanical Engineering,* 17(1), 2015, 7577-7586.
[21] Shahbakhsh, S., Tohidlou, E., Khosravi, H., Influence of modified carbonate calcium nanoparticles on the mechanical properties of carbon fiber/epoxy composites, *The Journal of the Textile Institute,* 111(4), 2020, 550-554.
[22] Ahmad, F., Yuvaraj, N., Bajpai, P.K., Effect of reinforcement architecture on the macroscopic mechanical properties of fiberous polymer composites: A review, *Polymer Composites,* 41(6), 2020, 2518-2534.
[23] Avrenli, K.A., Dempsey, B.J., A kinematic methodology to optimize the landing trajectory for the Boeing 737 jet undergoing total loss of thrust, *Journal of Transportation Safety & Security*, 9(1), 2017, 82-104.
[24] DeVault, T. L., Blackwell, B. F., Seamans, T. W., Belant, J. L., Identification of off airport interspecific avian hazards to aircraft, *The Journal of Wildlife Management,* 80(4), 2016, 746-752.
[25] Zekan, H.E., Haijun, X.U.A.N., Conger, B.A.I., Manli, S.O.N.G., Zhuoshen, Z.H.U., Containment of soft wall casing wrapped with Kevlar fabric, *Chinese Journal of Aeronautics,* 32(4), 2019, 954-966.
[26] Avrenli, K.A., Dempsey, B.J., 2015, A kinematic approach to segmented-trajectory generation for the total loss of thrust emergency, *Aviation,* 19(3), pp. 138-149.
[27] Randjbaran, E., Zahari, R., Jalil, N.A., Majid, D.L., Hybrid Composite laminates reinforced with kevlar/carbon/glass woven fabrics for ballistic impact testing, *The Scientific World Journal,* 2014, 2014, 413753.
[28] Bartoli, M., Giorcelli, M., Rosso, C., Rovere, M., Jagdale, P., Tagliaferro, A., Influence of commercial biochar fillers on brittleness/ductility of epoxy resin composites, *Applied Sciences,* 9(15), 2019, 3109.
[29] Randjbaran, E., Majid, D.L., Zahari, R., Sultan, M.T. and Mazlan, N., Effects of Volume of Carbon Nanotubes on the Angled Ballistic Impact for Carbon Kevlar Hybrid Fabrics, *Facta Universitatis, Series: Mechanical Engineering,* 18(2), 2020, 229-244.
[30] Pangh, H., Hosseinabadi, H.Z., Kotlarewski, N., Moradpour, P., Lee, M. and Nolan, G., 2019, Flexural performance of cross-laminated timber constructed from fibre-managed plantation eucalyptus, *Construction and Building Materials,* 208, pp. 535-542.
[31] ASTM D790-17, Standard Test Methods for Flexural Properties of Unreinforced and Reinforced Plastics and Electrical Insulating Materials, *ASTM International,* West Conshohocken, PA, 2017
[32] Yusof, N.S.B., Sapuan, S.M., Sultan, M.T.H. and Jawaid, M., Conceptual design of oil palm fibre reinforced polymer hybrid composite automotive crash box using integrated approach, *Journal of Central South University*, 27(1), 2020, 64-75.
[33] Mohsen, M.O., Taha, R., Taqa, A.A. and Shaat, A., Optimum carbon nanotubes' content for improving flexural and compressive strength of cement paste, *Construction and Building Materials*, 150, 2017, 395-403.

ORCID iD

Elias Randjbaran https://orcid.org/0000-0003-1202-5398
Dayang L. Majid https://orcid.org/0000-0001-6325-9341
Rizal Zahari https://orcid.org/0000-0002-3951-7619
Mohamed T. H. Sultan https://orcid.org/0000-0002-5110-0242
Norkhairunnisa Mazlan https://orcid.org/0000-0003-0144-8360

How to cite this article: Randjbaran E., Majid D.L., Zahari R., Sultan M.T.H., Mazlan N. Impacts of Volume of Carbon Nanotubes on Bending for Carbon-Kevlar Hybrid Fabrics, *J. Appl. Comput. Mech.*, 7(2), 2021, 839–848.
https://doi.org/10.22055/JACM.2020.35554.2682